HHS Public Access

Author manuscript

J Nutr Biochem. Author manuscript; available in PMC 2021 September 01.

Published in final edited form as:

J Nutr Biochem. 2021 September ; 95: 108764. doi:10.1016/j.jnutbio.2021.108764.

Adipocyte inducible 6-phosphofructo-2-kinase suppresses adipose tissue inflammation and promotes macrophage anti-inflammatory activation

Hang Xu[a,1], **Bilian Zhu**[a,b,1], **Honggui Li**[a,1], **Boxiong Jiang**[b], **Yina Wang**[b], **Qiongli Yin**[b], **James Cai**[c], **Shannon Glaser**[d], **Heather Francis**[e,f], **Gianfranco Alpini**[e,f], **Chaodong Wu**[a,*]

[a]Department of Nutrition, Texas A&M University, College Station, Texas, USA

[b]Department of VIP Medical Service Center, the Third Affiliated Hospital of Sun Yat-sen University, Guangzhou, Guangdong, China

[c]Department of Veterinary Integrative Biosciences, Texas A&M University, College Station, Texas, USA

[d]Medical Physiology, Texas A&M University College of Medicine, Bryan, Texas, USA

[e]Hepatology and Gastroenterology, Medicine, Indiana University, Indianapolis, Indiana, USA

[f]Richard L. Roudebush VA Medical Center, Indianapolis, Indiana, USA

Abstract

Obesity-associated inflammation in white adipose tissue (WAT) is a causal factor of systemic insulin resistance. To better understand how adipocytes regulate WAT inflammation, the present study generated chimeric mice in which inducible 6-phosphofructo-2-kinase was low, normal, or high in WAT while the expression of 6-phosphofructo-2-kinase/fructose-2,6-bisphosphatase 3 (*Pfkfb3*) was normal in hematopoietic cells, and analyzed changes in high-fat diet (HFD)-induced WAT inflammation and systemic insulin resistance in the mice. Indicated by proinflammatory signaling and cytokine expression, the severity of HFD-induced WAT inflammation in WT → *Pfkfb3*$^{+/-}$ mice, whose *Pfkfb3* was disrupted in WAT adipocytes but not hematopoietic cells, was comparable with that in WT → WT mice, whose *Pfkfb3* was normal in all cells. In contrast, the severity of HFD-induced WAT inflammation in WT → Adi-Tg mice, whose *Pfkfb3* was over-expressed in WAT adipocytes but not hematopoietic cells, remained much lower than that in WT → WT mice. Additionally, HFD-induced insulin resistance was correlated with the status of

*Corresponding author at: Chaodong Wu, 2253 TAMU, College Station, Texas 77843, USA. Fax: 979 862 7782, cdwu@tamu.edu (C. Wu).

[1]H.X., B.Z., and H.L. share the first authorship.

Author Contribution

H.X. B.Z., and H.L. carried out most of experiments involving mice. H.X. and H.L. carried out most of the experiments involving cells. H.X., B.Z., and H.L. collected tissue and cell samples and performed molecular and biochemical assays. H.L. performed histological assays. B.J., Y.W., Q.L., J.C., S.G., H.F., and G.A. contributed to scientific discussion. C.W. came up the concept of the study and supervised all experiments and wrote the manuscript.

Declaration of Competing Interests

The authors do not have conflict of interest.

Supplementary materials

Supplementary material associated with this article can be found, in the online version, at doi:10.1016/j.jnutbio.2021.108764.

WAT inflammation and comparable between WT → *Pfkfb3*$^{+/-}$ mice and WT → WT mice, but was significantly lower in WT → Adi-Tg mice than in WT → WT mice. *In vitro*, palmitoleate decreased macrophage phosphorylation states of Jnk p46 and Nfkb p65 and potentiated the effect of interleukin 4 on suppressing macrophage proinflammatory activation. Taken together, these results suggest that the *Pfkfb3* in adipocytes functions to suppress WAT inflammation. Moreover, the role played by adipocyte *Pfkfb3* is attributable to, at least in part, palmitoleate promotion of macrophage anti-inflammatory activation.

Keywords

Pfkfb3; Adipocytes; Adipose tissue inflammation; Insulin resistance; Palmitoleate

1. Introduction

Obesity is a causal factor of a wide variety of chronic diseases including type 2 diabetes, non-alcoholic fatty liver diseases, cardiovascular disease, and certain forms of cancer [1–5]. Over the past several decades, compelling evidence has demonstrated the interplays among fat deposition (*e.g.*, adiposity and hepatic steatosis), chronic low-grade inflammation, and insulin resistance as the mechanisms underlying how obesity causes chronic diseases. In particular, nutritional stress, such nutrient overload and unhealthy diet composition, is shown to trigger or exacerbate white adipose tissue (WAT) inflammation, which in turn critically contributes to the development of insulin resistance and insulin resistance-associated metabolic dysregulation [6–10].

Within WAT, both adipocytes and macrophages are essential for regulating the development and progression of inflammation. For example, nutritional stress triggers oxidative stress and/or endoplasmic reticulum stress in adipocytes [11–13]. This process increases adipocyte production of proinflammatory mediators including cytokines and chemokines and leads to inappropriate adipocyte-macrophage crosstalk, thereby exacerbating WAT inflammatory responses and metabolic dysfunctions [8,14]. In contrast, adipocytes also are capable of producing Th2 cytokines that function to promote macrophage alternative activation. The latter is anti-inflammatory and acts to protect against obesity-related insulin resistance and metabolic dysregulation [9]. More importantly, upon activation of peroxisome proliferator-activated receptor gamma (Pparg), adipocytes reveal decreased proinflammatory responses [15,16]. This likely explains decreased WAT inflammation that may or may not be accompanied with increased WAT macrophage accumulation [17,18] and accounts for the insulin-sensitizing effect of thiazolidinediones that have been used as anti-diabetic medicines to reverse insulin resistance [19–22]. Similar to its actions on adipocytes, nutritional stress causes hyperactivation of immune cells, in particular those in WAT. The latter contributes to the pathogenesis of WAT inflammation. For instance, feeding a high-fat diet (HFD) to C57BL/6 mice induces increased WAT macrophage accumulation and proinflammatory activation that are commonly accompanied with systemic insulin resistance [23–25], However, it remains to be elucidated precisely how, within WAT, adipocytes act through a paracrine manner to regulate macrophage activation status, and thereby WAT inflammation.

As a master regulatory gene whose product inducible 6-phosphofructo-2-kinase (iPfk2) functions to stimulate glycolysis, *Pfkfb3* is expressed at high abundance in adipocytes and acts to link adipocyte metabolic and inflammatory responses. For instance, *Pfkfb3* knockdown decreased adipocyte glycolysis, resulting in a compensatory increase in adipocyte fatty acid oxidation that contributed to increased production of reactive oxygen species and proinflammatory responses [15,23]. In contrast, overexpression of iPfk2 in adipocytes increased glycolysis and glycolysis-derived lipogenesis, resulting in decreased adipocyte production of reactive oxygen species and proinflammatory responses [26]. These findings explained, to a large extent, that *Pfkfb3* disruption increased and adipocyte-specific *Pfkfb3* overexpression decreased the severity of HFD-induced WAT inflammation and systemic insulin resistance [23,26]. However, in global *Pfkfb3*-disrupted mice, *Pfkfb3* was also disrupted in macrophages, whose activation status tightly regulates WAT inflammation. In contrast, in adipocyte-selective overexpressing mice, aP2-driven *Pfkfb3* overexpression likely also occurred in WAT immune cells, in particular macrophages. To more specifically determine a role for the *Pfkfb3* in adipocytes in regulating WAT inflammation, the present study analyzed WAT inflammation in relation to systemic insulin resistance using chimeric mice in which *Pfkfb3*/iPfk2 was low, normal, or high in WAT adipocytes, but normal in WAT immune cells. The results suggest that adipocyte *Pfkfb3* plays a critical role in suppressing WAT inflammation. Also, this role of adipocyte *Pfkfb3* involves palmitoleate.

2. Materials and methods

2.1. Animal experiments

C57BL/6J mice were originally obtained from Jackson Laboratory (Bar Harbor, ME). Global heterozygous *Pfkfb3*-disrupted (*Pfkfb3*$^{+/-}$) mice and adipocyte-specific *Pfkfb3*-overexpressing (Adi-Tg) mice, as well as their wild-type (WT) littermates were generated and maintained as described [23,26]. All mice were maintained on a 12:12-h light-dark cycle (lights on at 06:00), and fed *ad libitum* except those that were used for dietary feeding studies. Some *Pfkfb3*$^{+/-}$ mice and Adi-Tg mice were used for generation of chimeric mice as described below to create WAT environment where *Pfkfb3* was disrupted or over-expressed in adipocytes but unchanged in hematopoietic cells. Study 1 (Effect of *Pfkfb3* disruption on WAT inflammation): Since homozygous *Pfkfb3* disruption is embryonic lethal [27], male *Pfkfb3*$^{+/-}$ mice and their WT littermates, at 5–6 wk of age, were fed an HFD (60% fat calories, 20% carbohydrate calories, and 20% protein calories; Research Diets, Inc.) for 12 wk as described [23]. Study 2 (Effect of adipocyte-specific *Pfkfb3* overexpression on WAT inflammation): Male Adi-Tg mice and their WT littermates, at 5–6 wk of age, were fed an HFD for 12 wk as described [26]. Most outcomes from Studies 1 and 2 have been previously reported [23,26]. Study 3 (Effect of decreased or increased adipocyte iPfk2 in the presence of WT *Pfkfb3* in hematopoietic cells on WAT inflammation): Within WAT of *Pfkfb3*$^{+/-}$ mice, *Pfkfb3* was also decreased in WAT immune cells, in particular macrophages that critically determine the inflammatory status of WAT. In contrast, within WAT of Adi-Tg mice, *Pfkfb3* expression was likely also increased in WAT macrophages in response to aP2 promoter-driven gene expression. Considering this, the present study generated WT → *Pfkfb3*$^{+/-}$ mice and WT → Adi-Tg mice, as well as WT → WT mice, using bone marrow transplantation (BMT) as described [24,28]. In these three types of chimeric mice, WAT

contained low, normal, or high amount of iPfk2 in adipocytes, but normal (WT) *Pfkfb3* in hematopoietic cells. These chimeric mice, after recovery from BMT, were fed an HFD for 12 wk identical to the mice in Studies 1 and 2. During feeding period, body weight was recorded weekly and food consumption was documented and used to calculate food intake. After the feeding period, the mice in Studies 1 through 3 were fasted for 4 h prior to collection of blood and tissue samples [15,28]. Epididymal, mesenteric, and perinephric fat depots were dissected and weighed as visceral fat content [23,25]. After weighing, part of the WAT was either fixed and embedded for histological and immunohistochemical analyses or frozen in liquid nitrogen and then stored at −80°C for further analyses. Some male WT mice were fed *ad libitum* and subjected to isolation of bone marrow cells for BMT or differentiation into macrophages for further analyses as described below. All study protocols were reviewed and approved by the Institutional Animal Care and Use Committee of Texas A&M University.

2.2. Isolation of bone marrow cells and differentiation of macrophages

Bone marrow cells were isolated from the tibias and femurs of WT C57BL/6J mice, at 10–12 wk of age as described [24,28]. After erythrocyte lysis with ammonium chloride (Stem Cell Technologies), the remaining cells were either used for BMT or induced for differentiation with Iscove's modified Dulbecco's medium containing 10% fetal bovine serum and 15% L929 culture supernatant for 8 d. The bone marrow-derived macrophages (BMDMs) were further analyzed for its activation status.

2.3. Bone marrow transplantation

At 5–6 wk of age, male recipients (*Pfkfb3*$^{+/-}$ mice, Adi-Tg mice, and WT littermates) were subjected to x-ray irradiation at a lethal dose. Immediately after irradiation, the recipients were transplanted with freshly isolated bone marrow cells from WT mice as described above. In WT → *Pfkfb3*$^{+/-}$ mice, *Pfkfb3* was disrupted in WAT adipocytes, but normal in hematopoietic cells. In WT → Adi-Tg mice, *Pfkfb3* was over-expressed in WAT adipocytes, but normal in hematopoietic cells. In WT → WT mice, *Pfkfb3* was normal in both adipocytes and hematopoietic cells.

2.4. Glucose and insulin tolerance tests

Glucose and insulin tolerance tests (GTT and ITT) were performed as described [29]. After the feeding period, mice were fasted for 4 h and received an intraperitoneal injection of D-glucose (2 g/kg of body weight) or insulin (1 unit/kg of body weight). For GTT, blood samples (5 μL) were collected from the tail vein before and at 30, 60, 90, and 120 min post the glucose bolus injection. Similarly, for ITT, blood samples were collected from the tail vein before and at 15, 30, 45, 60 min post the bolus insulin injection. Area under curve (AUC) was calculated based on the data from GTT and ITT [30].

2.5. Measurement of plasma levels of glucose and insulin

The levels of plasma glucose were measured using a glucose assay kit (Sigma-Aldrich, St Louis, MO). The levels of plasma insulin were measured using an ELISA kit (Crystal Chem Inc., Downers Grove, IL).

2.6. Histological and immunohistochemical analyses

Paraffin-embedded mouse WAT blocks were cut into sections of 5 μm thickness and stained with hematoxylin and eosin (H&E) and/or stained for F4/80 expression with rabbit anti-F4/80 antibodies (1:1,000) (AbD Serotec, Raleigh, NC) [29,31].

2.7. Analysis of adipocyte size and number

Images of H&E stained adipose tissue sections were analyzed using Adiposoft of Image J software. Three fields of view for slides of WAT from seven mice per group were quantified. The quantification unit of pixels were converted to microns using the following formula: 1 pixel=0.645 μm at × 10 objective. Adipocyte number per field was calculated for adipocytes with a diameter ranging from 20–2000 μm during automated analysis. The size distribution (frequency) of adipocytes was calculated based on adipocyte size and number obtained, and plotted using the Excel Software.

2.8. Adipose tissue insulin signaling

After the feeding period, some mice from Studies 1 through 3 were fasted for 4 h and received a bolus injection of insulin (1 unit/kg body weight) into the portal vein for 5 min prior to harvest. WAT lysates were examined for the total amount and phosphorylation states of Akt1/2 using Western blot analysis.

2.9. Isolation of WAT adipocytes and stromal cells

Adipocytes and stromal cells were isolated from WAT in chimeric mice using the collagenase digestion method as previously described [24,28]. After digestion and centrifugation, the floating cells and pelleted cells were collected as adipocytes and stromal cells, respectively. The isolated cells were examined for *Pfkfb3* mRNAs as described in cellular and molecular assays. Additional stromal cells were subjected to FACS analyses using flowcytometry described [24,28].

2.10. Cell culture and treatment

Stable iPfk2-overexpressing adipocytes and green fluorescent protein-expressing adipocytes (control) were established and maintained as described [15]. Adipocyte-conditioned media were collected at 8 d post differentiation and subjected to determination of the abundance of palmitoleate as described [26,30]. Next, the effect of palmitoleate on macrophage activation was analyzed. After differentiation, BMDMs were treated with palmitoleate (50 μ*M*, conjugated with 10% bovine serum albumin (BSA)), palmitate (250 μM), or BSA for 24 h prior to harvest. Additional BMDMs were treated with Pal (250 μ*M*) or PO (50 or 250 μM) for 24 h in the presence of LPS for the last 30 min. Cell lysates were examined for the total amount and phosphorylation states of c-Jun kinase (Jnk) p46 and nuclear factor kappa B (Nfkb) p65 using Western blot analysis while some cells were harvested for RNA samples and examined for the expression of inflammatory mediators using real-time RT-PCR. To analyze the effect of PO on macrophage alternative activation, portions of BMDMs were incubated with or without interleukin 4 (Il4, 10 ng/mL) for 48 h in the presence or absence of PO (50 μM) for the last 24 h. Prior to harvest, the cells were also treated with or without LPS (100 ng/mL) for the last 30 min. Cell lysates were examined for the total amount and

phosphorylation states of Jnk p46 and Nfkb p65 using Western blot analysis. Additional BMDMs were treated with Il4 and/or PO identically and examined for the expression of proinflammatory cytokines and anti-inflammatory mediators (*Tnfa, Il1b, Il6, arginase 1* (*Arg1*), *Il10*, and *Pparg*).

2.11. Biochemical and molecular assays

The amount of iPfk2 in WAT and/or the mRNA levels of *Pfkfb3* in BMDMs or isolated WAT cells from the mice of Studies 1 through 3 were determined using Western blot analysis and real-time PCR, respectively, as described [15,29]. To determine WAT and BMDM proinflammatory signaling and WAT insulin signaling, lysates of frozen WAT or cultured cells were subjected to Western blot analysis as described [31,32]. All primary antibodies were from Cell Signaling Technology (Danvers, MA, USA). The maximum intensity of each band was quantified using ImageJ software. To determine gene expression, the total RNA was isolated from cultured/isolated cells and subjected to reverse transcription and real-time PCR analysis. Results were normalized to 18s ribosomal RNA and plotted as relative expression to the average of WT, basal WT, or WT → WT, which was set as 1.

2.12. Statistical methods

Numeric data are presented as means ± standard error (SEM). Statistical significance was determined using unpaired, two-tailed ANOVA or Student's *t* tests. Differences were considered significant at the two-tailed $P < .05$.

3. Results

3.1. *Adoptive transfer of WT hematopoietic cells to* Pfkfb3-*disrupted or selective* Pfkfb3-*overexpressing mice does not alter adipose tissue amount of iPfk2*

Pfkfb3-disrupted (*Pfkfb3*$^{+/-}$) mice revealed decreased WAT amount of iPfk2, due to *Pfkfb3* disruption in both adipocytes and WAT immune cells [23,27]. In contrast, selective *Pfkfb3*-overexpressing mice (Adi-Tg) mice revealed increased WAT amount of iPfk2 [26]. Using these two lines of mice (Fig. 1A), we generated chimeric mice in which immunes cells contained WT *Pfkfb3*. These resultant chimeric mice were expected to have decreased or increased iPfk2 in adipocytes, but not WAT immune cells, and were used for studying obesity-related WAT inflammation and systemic insulin resistance. After harvesting of chimeric mice, we verified that WAT iPfk2 amount was lower in WT → *Pfkfb3*$^{+/-}$ mice and higher in WT → Adi-Tg mice than that in WT → WT mice whereas *Pfkfb3* mRNA levels in BMDMs from all chimeric mice were comparable (Fig. 1B, C). Among the isolated cells, WAT adipocytes from WT → Adi-Tg mice revealed markedly higher *Pfkfb3* mRNAs whereas adipocytes from WT → *Pfkfb3*$^{+/-}$ mice revealed significantly decreased *Pfkfb3* mRNAs compared with those from WT → WT mice; although stromal cells from WT → Adi-Tg mice displayed slightly increased *Pfkfb3* mRNAs (Fig. 1D). Therefore, adoptive transfer of WT hematopoietic cells to recipients did not alter WAT iPfk2 amount, which enabled us to study the role of altering adipocyte iPfk2 in the regulation of WAT inflammation and systemic insulin resistance.

3.2. The iPfk2 in adipocytes, but not hematopoietic cells, determines body weight and adiposity

Pfkfb3/iPfk2 plays a critical role in regulating diet-induced adiposity and adipocyte size [23,26]. Consistently, the size of adipocytes in HFD-fed *Pfkfb3*$^{+/-}$ mice was significantly smaller than that in WT mice (Supplemental Figure S1). In contrast, the size of adipocytes in HFD-Adi-Tg mice was significantly larger than that in HFD-WT (Supplemental Figure S1). These features were not significantly altered by adoptive transfer of WT hematopoietic cells to *Pfkfb3*$^{+/-}$ mice and/or Adi-Tg mice. Specifically, upon HFD feeding, WT → *Pfkfb3*$^{+/-}$ mice revealed a smaller gain of body weight compared with WT → WT mice whereas WT → Adi-Tg mice displayed a significantly more gain of body weight (Fig. 2A). In addition, HFD-fed WT → *Pfkfb3*$^{+/-}$ mice displayed significantly decreased and HFD-fed WT → Adi-Tg displayed significantly increased visceral fat mass and adiposity compared with HFD-fed WT → WT mice (Fig. 2B). When compared with *Pfkfb3*$^{+/-}$ mice, WT → *Pfkfb3*$^{+/-}$ mice did not reveal significant differences in body weight before and after HFD feeding, and displayed nearly similar patterns of visceral fat mass and adiposity in response to HFD feeding (Supplemental Figure S2A, B, C). When compared with Adi-Tg mice, WT → Adi-Tg mice also did not reveal significant differences in body weight before and after HFD feeding, and displayed nearly similar patterns of visceral fat mass and adiposity upon HFD feeding (Supplemental Figure S2D, E, F). Consistently, the size of WAT adipocytes was smaller in HFD-fed WT → *Pfkfb3*$^{+/-}$ mice and larger in HFD-fed WT → Adi-Tg mice than that in HFD-fed WT → WT mice (Fig. 2C, D). In addition, the average numbers of adipocyte per field of WAT sections were much greater in HFD-fed WT → *Pfkfb3*$^{+/-}$ mice and much smaller in HFD-fed WT → Adi-Tg mice than those in HFD-fed WT → WT mice (Fig. 2D). Changes in adipocyte size also were reflected by distribution of adipocyte size (frequency) (Fig. 2E), indicating that there were more small adipocytes and fewer large adipocytes of WAT in HFD-fed WT → *Pfkfb3*$^{+/-}$ mice whereas there were fewer small adipocytes and more large adipocytes of WAT in HFD-fed WT → Adi-Tg mice than those, respectively, in HFD-fed WT → WT mice (Fig. 2C,D). During the feeding period, all chimeric mice consumed a comparable amount of food intake (data not shown). Together, these results validated that the *Pfkfb3*/iPfk2 in adipocytes, but not hematopoietic cells, critically regulates adipose tissue mass or adiposity.

3.3. *Adoptive transfer of wild-type hematopoietic cells to recipients does not weaken the effect of aP2-driven* Pfkfb3 *overexpression on ameliorating the severity of HFD-induced WAT inflammation*

Pfkfb3 disruption exacerbated whereas aP2-driven *Pfkfb3* overexpression ameliorated the severity of HFD-induced WAT inflammation [23,26]. To verify a role for iPfk2 in adipocytes and rule out roles for iPfk2 in immune cells in regulating WAT inflammation, we examined WAT inflammation in the chimeric mice. Indicated by F4/80-positive cells in WAT sections, the degree of macrophage accumulation in WT → *Pfkfb3*$^{+/-}$ mice was comparable with that in WT → WT mice (Fig. 3A). In contrast, the degree of WAT macrophage accumulation in WT → Adi-Tg mice was greater than that in WT → WT mice; however, this was accompanied with decreased WAT proinflammatory signaling and cytokine expression, as well as increased percentages of alternative (M2) macrophages among WAT stromal cells (below).

Next, the present study examined WAT inflammatory signaling and cytokine expression. HFD-induced phosphorylation states of Nfkb p65 and mRNA levels of proinflammatory cytokines and inflammatory mediators (*Tnfa, Il1b, Il6, Mcp1*, and *Il10*) in WT → *Pfkfb3*$^{+/-}$ mice were comparable with their respective levels in WT → WT mice; although the phosphorylation states of Jnk p46 in WT → *Pfkfb3*$^{+/-}$ mice were higher than those in WT → WT mice (Fig. 3B, C). In contrast, the phosphorylation states of Jnk p46 and Nfkb p65 and the mRNA levels of *Tnfa, Il1b*, and *Mcp1* in HFD-fed WT → Adi-Tg mice were significantly lower than their respective levels in WT → WT mice (Fig. 3B, C). When macrophage activation status was analyzed, the percentages of alternative (M2) macrophages among stromal cells from WAT in WT → Adi-Tg mice were significantly higher than those in WT → WT mice (Fig. 3D). Taken together, these results indicate that adoptive transfer of WT hematopoietic cells to Adi-Tg mice did not significantly alter the effect of aP2-driven *Pfkfb3* overexpression on ameliorating the severity of HFD-induced WAT inflammation while the same transfer alleviated the effect of *Pfkfb3* disruption on increasing the severity of HFD-induced WAT inflammation.

3.4. *Palmitoleate functions as a* Pfkfb3*-driven adipocyte bioactive lipid to promote macrophage anti-inflammatory activation*

Pfkfb3 overexpression increased the levels of palmitoleate in WAT and in adipocyte-conditioned media (Supplemental Figure S3) as reported previously [26]. Next, the present study examined the direct effects of palmitoleate on macrophage activation. In cultured BMDMs, treatment with palmitate caused a significant increase in the phosphorylation states of Jnk p46 and Nfkb p65. In contrast, treatment of BMDMs with palmitoleate nearly abolished the phosphorylation states of Jnk p46 and significantly decreased the phosphorylation states of Nfkb p65 (Fig. 4A). Under LPS-stimulated conditions, palmitoleate also significantly decreased the phosphorylation states of Jnk p46; although revealing limited effect on decreasing the phosphorylation states of Nfkb p65. Importantly, treatment of BMDMs with palmitoleate potentiated the effect of Il4, a key stimulator of macrophage alternative activation, on decreasing the phosphorylation states of Jnk p46 and Nfkb p65 (Fig. 4B). When macrophage gene expression was examined, treatment with palmitoleate significantly decreased or potentiated the effect of Il4 on decreasing macrophage mRNA levels of *Tnfa, Il1b*, and *Il6* while revealing marginal effect on increasing the mRNA levels of Il10 or *Arg1* (Fig. 4C). Since PO and Pal displayed the opposite effects on macrophage proinflammatory signaling under die basal condition (in the absence of LPS), we next examined the effects of PO vs. Pal (at a dose of 250 μM) on altering LPS-stimulated macrophage proinflammatory responses. As expected, treatment of BMDMs with PO caused significant decreases in LPS-stimulated phosphorylation states in Jnk p46 and Nfkb p65 compared with treatment of BMDMs with Pal (Fig. 4D, quantitative data not shown). At a same dose, PO also significantly decreased the mRNAs of *Tnfa* and *Il1b* while increased the mRNAs of *Arg1* and *Pparg* compared with palmitate (Fig. 4E). Together, these results suggest that PO, as a *Pfkfb3*-driven adipocyte bioactive lipid, functions to promote macrophage anti-inflammatory activation.

3.5. *Adoptive transfer of wild-type hematopoietic cells to recipients does not weaken the effect of aP2-driven* Pfkfb3 *overexpression on ameliorating the severity of HFD-induced systemic insulin resistance and glucose intolerance*

Pfkfb3 disruption exacerbated whereas aP2-driven *Pfkfb3* overexpression ameliorated the severity of HFD-induced systemic insulin resistance and glucose intolerance [23,26]. These phenotype differences were further confirmed by quantitative data presented as area under curve (AUC) (Supplemental Figure S4). Next, we sought to examine whether these phenotypes were altered by adoptive transfer of WT hematopoietic cells. The severity of HFD-induced systemic insulin resistance and glucose intolerance in WT → *Pfkfb3*$^{+/-}$ mice was comparable with that in WT → WT mice. In contrast, the improvement of systemic insulin sensitivity and glucose tolerance in HFD-fed WT → Adi-Tg mice relative to WT → WT mice was comparable to that in HFD-fed Ad-Tg mice relative to HFD-fed WT mice (Fig. 5A, B; Supplemental Figure S4). Among three groups of chimeric mice, the levels of plasma glucose were comparable (Fig. 5C). However, the levels of plasma insulin in HFD-fed WT → Adi-Tg mice were significantly lower than those in HFD-fed WT → WT mice, as well as HFD-fed WT → *Pfkfb3*$^{+/-}$ mice (Fig. 5D). Together, these results indicated that adoptive transfer of WT hematopoietic cells to Ad-Tg mice in gain-of-function study did not alter the effect of aP2-driven *Pfkfb3* overexpression on ameliorating the severity of HFD-induced systemic insulin resistance and glucose intolerance while the same transfer in loss-of-function study weakened the effect of *Pfkfb3* disruption on exacerbating HFD-induced metabolic phenotype. In addition, when compared with *Pfkfb3*$^{+/-}$ mice, WT → *Pfkfb3*$^{+/-}$ mice revealed significantly decreased (improved) severity of HFD-induced systemic insulin resistance and glucose intolerance (Supplemental Figure S5A,B). In contrast, WT → Adi-Tg mice displayed comparable degrees in systemic insulin sensitivity and glucose tolerance relative to Ad-Tg mice (Supplemental Figure S5C,D). These results suggest that replacement of *Pfkfb3*-disrupted hematopoietic cells, but not hematopoietic cells from aP2-*Pfkfb3*-overexpressing mice, with WT hematopoietic cells altered HFD-induced insulin resistance, validating the importance of the intact *Pfkfb3* in hematopoietic cells in regulating metabolic homeostasis [29].

3.6. *Adoptive transfer of wild-type hematopoietic cells to recipients does not weaken the effect of aP2-driven* Pfkfb3 *overexpression on increasing WAT insulin signaling*

HFD-induced WAT inflammation is commonly accompanied with decreased WAT insulin signaling. In HFD-fed *Pfkfb3*$^{+/-}$ mice, insulin-stimulated phosphorylation states of Akt were significantly lower than those in HFD-fed WT mice (Supplemental Figure S6A, quantitative data were based on blots in a previously published study [23]). In contrast, insulin-stimulated phosphorylation states of Akt in HFD-fed Adi-Tg mice were significantly higher than those in HFD-fed WT mice (Supplemental Figure S6B, quantitative data were based on blots in a previously published study [26]). When WAT insulin signaling was analyzed in chimeric mice, insulin-stimulated phosphorylation states of Akt in HFD-fed WT → *Pfkfb3*$^{+/-}$ mice did not differ significantly from those in HFD-fed WT → WT mice. However, insulin-stimulated Akt phosphorylation states in HFD-fed WT → Adi-Tg remained significantly higher than those in HFD-fed WT → WT mice (Fig. 6). These results indicate that adoptive transfer of WT hematopoietic cells to Adi-Tg mice did not weaken the effect of aP2-driven *Pfkfb3* overexpression on increasing WAT insulin signaling while

the same transfer blunted the effect of *Pfkfb3* disruption on exacerbating HFD-induced WAT insulin resistance.

4. Discussion

While stimulating adipocyte glycolysis and glycolysis-derived lipogenesis, *Pfkfb3* critically determines the severity of HFD-induced adiposity [23,26]. This role appears to be attributable to the *Pfkfb3* in adipocytes, but not immune cells. In support of this, adoptive transfer of WT hematopoietic cells to *Pfkfb3*$^{+/-}$ mice did not significantly influence the effect of *Pfkfb3* disruption on decreasing HFD-induced weight gain and adiposity. As complementary evidence, adoptive transfer of WT hematopoietic cells to Adi-Tg mice also did not significantly influence the effect of aP2-driven *Pfkfb3* overexpression on increasing the degrees of HFD-induced weight gain and adiposity. These findings strongly suggest that the *Pfkfb3* in hematopoietic cells has a limited role in regulating HFD-induced adiposity, which is consistent with the finding in a study involving myeloid-specific *Pfkfb3*-deficient mice whose body weight and adiposity were comparable with those in control mice upon HFD feeding [29]. However, the presence of WT *Pfkfb3* in WAT immune cells in the chimeric mice where *Pfkfb3* was disrupted or over-expressed in adipocytes had enabled us to better examine the role of adipocyte *Pfkfb3* in regulating WAT inflammation, as well as local and systemic insulin sensitivity (see below).

In terms of regulating WAT inflammation, we reported before that *Pfkfb3* disruption exacerbated HFD-induced WAT inflammation [23]. Since *Pfkfb3* is expressed at high abundance in both adipocytes and macrophages, we postulated that *Pfkfb3* disruption-driven increases in proinflammatory responses in both adipocytes and WAT macrophages contributed to increased severity of HFD-induced WAT inflammation in *Pfkfb3*$^{+/-}$ mice. According to this postulation, adoptive transfer of WT hematopoietic cells to global *Pfkfb3*-disrupted mice would alleviate the severity of HFD-induced WAT inflammation due to replacement of *Pfkfb3*-disrupted hematopoietic cells with WT cells and this was verified to be true. More specifically, the severity of HFD-induced WAT inflammation, indicated by the phosphorylation states of Nfkb p65 and the mRNA levels of *Il1b*, *Il6*, Il10, *Tnfa*, and *Mcp1*, was comparable between WT → *Pfkfb3*$^{+/-}$ mice and WT → WT mice. Because of this, the *Pfkfb3* in hematopoietic cells appears to play a more important role than that in adipocytes in protecting against HFD-induced WAT inflammation. As a logical step, we also performed adoptive transfer of WT hematopoietic cells to Adi-Tg mice with hope to rule out the extent to which, in the gain-of-function study, aP2-driven *Pfkfb3* expression in the cells other than adipocytes, in particular WAT immune cells, contributed to decreased severity of HFD-induced WAT inflammation. In other words, we also postulated that adoptive transfer of WT hematopoietic cells to Adi-Tg mice would weaken the effect of aP2-driven *Pfkfb3* overexpression on decreasing the severity of HFD-induced WAT inflammation. However, this was not the case; given that the degree of HFD-induced WAT inflammation in WT → Adi-Tg mice was much smaller than that in WT → WT mice. Why adoptive transfer of WT bone marrow cells did not weaken the effect of aP2-driven *Pfkfb3* overexpression on decreasing WAT inflammation was likely due to that aP2-driven *Pfkfb3* overexpression in macrophages, if existing, was at low levels and not sufficient enough to further decrease HFD-induced severity of WAT inflammation that was already

low due to *Pfkfb3* overexpression in adipocytes. Alternatively, within WAT of WT → Adi-Tg mice, WT hematopoietic cells, in particular macrophages, responded to *Pfkfb3* overexpression-driven adipocyte factors and produced anti-inflammatory effects comparable with those caused by aP2-driven *Pfkfb3* overexpression in WAT macrophages. Regardless, decreased phenotype in HFD-induced WAT inflammation in WT → Adi-Tg mice relative to WT → WT mice strongly suggests a critical role for adipocyte *Pfkfb3*, at increased levels or activities, in suppressing WAT inflammation.

Suppression of WAT inflammation by adipocyte *Pfkfb3* involves palmitoleate. As it has been illustrated before, *Pfkfb3* stimulates adipocyte glycolysis and increases the conversion of glucose to lipids [26]. This property enables *Pfkfb3* to promote adipocyte production of palmitoleate, which functions as a bioactive lipid to exhibit anti-inflammatory effects. In fact, several previous studies have validated that treatment of macrophages (RAW264.7 cells) with palmitoleate decreased the phosphorylation states of Nfkb p65 and the mRNA levels of *Tnfa* and *Il6* [30]. Similarly, treatment of BMDMs with palmitoleate decreased the effect of LPS on stimulating the expression of proinflammatory cytokines at both mRNA and protein levels [33]. While exploring nutrition stress-related macrophage polarization, the study by Chan et al. revealed that treatment of BMDMs with palmitoleate increased anti-inflammatory genes (*Mrc1*, *Tgfb1*, *Il10*, and *Mgl2*) and oxidative metabolism, suggesting increased macrophage M2 activation [34]. In the present study, we validated that treatment with palmitoleate significantly decreased macrophage phosphorylation states of Jnk p46 and Nfkb p65. Moreover, palmitoleate appeared to potentiate the effects of Il4, an essential stimulator needed for macrophage M2 activation, on decreasing macrophage phosphorylation states of Jnk p46 and Nfkb p65, as well as expression of *Il1b*. Based on these findings, we argue in favor that palmitoleate, as a *Pfkfb3*-dnven adipocyte factor, functions to suppress macrophage proinflammatory activation. This effect of palmitoleate is expected to contribute to decreased WAT inflammation in WT → Adi-Tg mice relative to WT → WT mice.

Pfkfb3 also regulates systemic insulin sensitivity while controlling adiposity and WAT inflammation. Of note, *Pfkfb3* dissociates obesity-associated insulin resistance from adiposity [23,26]. In contrast, *Pfkfb3* regulation of insulin sensitivity is closely associated with its control of WAT inflammation. Specifically, *Pfkfb3* disruption increased WAT inflammation and insulin resistance whereas selective *Pfkfb3* overexpression decreased WAT inflammation and insulin resistance. This role played by *Pfkfb3* is attributable to cell-specific roles for *Pfkfb3* in regulating different events related to obesity. As discussed above, HFD-induced adiposity was closely regulated by the *Pfkfb3* in adipocytes, but not hematopoietic cells. In terms of regulating systemic and local (WAT) insulin sensitivity, however, the *Pfkfb3* in both adipocytes and hematopoietic cells accounts for suppressing the effect of nutrition stress, *e.g.*, HFD feeding, on inducing insulin resistance. As supporting evidence, the degrees of local and systemic insulin sensitivity in HFD-fed WT → $Pfkfb3^{+/-}$ mice were comparable with those in HFD-fed WT → WT mice. This suggests that adoptive transfer of WT hematopoietic cells to $Pfkfb3^{+/-}$ mice was sufficient to weaken or even blunt the effect of (heterozygous) *Pfkfb3* disruption on increasing HFD-induced local and systemic insulin resistance. In contrast, in the gain-of-function study involving Adi-Tg mice, the degrees of HFD-induced local and systemic insulin resistance in WT → Adi-Tg mice

remained much smaller than those in WT → WT mice, supporting that selective *Pfkfb3* overexpression in adipocytes was sufficient to alleviate or blunt the effect of HFD feeding on inducing local and systemic insulin resistance. Taken together, these findings validate that the *Pfkfb3* in both adipocytes and hematopoietic cells reveals a role in protecting against HFD-induced insulin resistance. Interestingly, in WT → *Pfkfb3*$^{+/-}$ mice, why *Pfkfb3* disruption in cells other hematopoietic cells, *e.g.*, adipocytes, was not sufficient to counter the insulin-sensitizing effect brought about adoptive transfer of WT hematopoietic cells remains to be investigated.

In summary, the present study provides evidence to support a critical role for *Pfkfb3* in adipocytes in protecting against obesity-associated WAT inflammation and systemic insulin resistance. The notable finding is that maintaining *Pfkfb3* overexpression only in adipocytes by adoptive transfer of WT hematopoietic cells to Adi-Tg mice did not significantly weaken the effects of aP2-driven *Pfkfb3* overexpression on decreasing or preventing HFD-induced WAT inflammation, as well as local and systemic insulin resistance. As a *Pfkfb3*-driven adipocyte factor, palmitoleate acted to promote macrophage anti-inflammatory activation, which likely accounted for decreased WAT inflammation and local and systemic insulin resistance in chimeric mice where *Pfkfb3* overexpression occurred only in adipocytes. As such, the *Pfkfb3* in adipocytes plays a unique role in regulating obesity-associated pathophysiological events.

Supplementary Material

Refer to Web version on PubMed Central for supplementary material.

Funding

This work was supported in part by the Hickam Endowed Chair, Gastroenterology, Medicine, Indiana University and the Indiana University Health - Indiana University School of Medicine Strategic Research Initiative (G.A. and H.F.), the Senior Research Career Scientist to G.A, and the NIH grants DK054811 and DK110035 to G.A. and S. G. and the NIH grant DK119421 to H.F. In addition, this work was supported in whole or in part by grants from the American Diabetes Association (1-10-BS-76 to C.W.) and NIH (DK095828 and DK124854 to C.W.). C.W. is also supported by the Hatch Program of the National Institutes of Food and Agriculture (NIFA).

Abbreviations:

BMDM	bone marrow-derived macrophages
BMT	bone marrow transplantation
Dulbecco's	modified Eagle's medium
FBS	fetal bovine serum
Gapdh	glyceraldehyde 3-phosphate dehydrogenase
H&E	hematoxylin and eosin
HFD	high-fat diet
Jnk	c-Jun N-terminal kinase

Il1b	interleukin 1 beta
Il4	interleukin 4
Il6	interleukin 6
iPfk2	inducible 6-phosphofructo-2-kinase
IMDM	Iscove's Modified Dulbecco's medium
LPS	lipopolysaccharide
Nfkb	nuclear factor kappa B
Pfkfb3	6-phosphofructo-2-kinase/fructose-2,6-biphosphatase 3
Pp46	phosphorylated p46 of c-Jun N-terminal kinase
Pp65	phosphorylated p65 subunit of Nfkb
Pparg	peroxisome proliferator-activated receptor gamma
ROS	reactive oxygen species
Tfna	tumor necrosis factor alpha
WAT	white adipose tissue
WT	wild-type

References

[1]. Pérez-Pevida B, Díaz-Gutiérrez J, Miras AD, Silva C, Romero S, Salvador J, et al.High body adiposity drives glucose intolerance and increases cardiovascular risk in normoglycemic subjects. Obesity2018;26:672–82. [PubMed: 29522277]

[2]. Ota T, Takamura T, Kurita S, Matsuzawa N, Kita Y, Uno M, et al.Insulin resistance accelerates a dietary rat model of nonalcoholic steatohepatitis. Gastroenterology2007;132:282–93. [PubMed: 17241878]

[3]. Fantuzzi G, Mazzone T. Adipose tissue and atherosclerosis: exploring the connection. Arterioscler Thromb Vasc Biol2007;27:996–1003. [PubMed: 17303782]

[4]. Caldwell SH, Crespo DM, Kang HS, Al-Osaimi AMS. Obesity and hepatocellular carcinoma. Gastroenterology2004;127:S97–S103. [PubMed: 15508109]

[5]. Botchlett R, Woo S-L, Liu M, Pei Y, Guo X, Li H, et al.Nutritional approaches for managing obesity-associated metabolic diseases. J Endocrinol2017;233:R145–RR71. [PubMed: 28400405]

[6]. Xu H, Barnes GT, Yang Q, Tan G, Yang D, Chou CJ, et al.Chronic inflammation in fat plays a crucial role in the development of obesity-related insulin resistance. J Clin Invest2003;112:1821–30. [PubMed: 14679177]

[7]. Greenberg AS, Obin MS. Obesity and the role of adipose tissue in inflammation and metabolism. Am J Clin Nutr2006;83461S–4615. [PubMed: 16470013]

[8]. Kamei N, Tobe K, Suzuki R, Ohsugi M, Watanabe T, Kubota N, et al.Overexpression of monocyte chemoattractant protein-1 in adipose tissues causes macrophage recruitment and insulin resistance. J Biol Chem2006;281:26602–14. [PubMed: 16809344]

[9]. Kang K, Reilly SM, Karabacak V, Gangl MR, Fitzgerald K, Hatano B, et al.Adipocyte-derived Th2 cytokines and myeloid PPARd regulate macrophage polarization and insulin sensitivity. Cell Metab2008;7:485–95. [PubMed: 18522830]

[10]. Shoelson SE, Herrera L, Naaz A. Obesity, inflammation, and insulin resistance. Gastroenterology2007;132:2169–80. [PubMed: 17498510]

[11]. Evans JL, Goldfine ID, Maddux BA, Grodsky GM. Oxidative stress and stress-activated signaling pathways: a unifying hypothesis of type 2 diabetes. Endocr Rev2002;23:599–622. [PubMed: 12372842]

[12]. Talior I, Tennenbaum T, Kuroki T, Eldar-Finkelman H. PKC-d-dependent activation of oxidative stress in adipocytes of obese and insulin-resistant mice: role for NADPH oxidase. Am J Physiol Endocrinol Metab2005;288:E405–11. [PubMed: 15507533]

[13]. Bai J, Cervantes C, Liu J, He S, Zhou H, Zhang B, et al.DsbA-L prevents obesity-induced inflammation and insulin resistance by suppressing the mtDNA release-activated cGAS-cGAMP-STING pathway. Proc Natl Acad Sci USA. 2017;114:12196–201. [PubMed: 29087318]

[14]. Meijer K, de Vries M, AI-Lahham S, Bruinenberg M, Weening De, Dijkstra M, et al.Human primary adipocytes exhibit immune cell function: adipocytes prime inflammation independent of macrophages. PLoS ONE2011;6:e17154. [PubMed: 21448265]

[15]. Guo X, Xu K, Zhang J, Li H, Zhang W, Wang H, et al.Involvement of inducible 6-phosphofructo-2-kinase in the anti-diabetic effect of PPARg activation in mice. J Biol Chem2010;285:23711–20. [PubMed: 20498376]

[16]. Moreno-Navarrete JM, Ortega F, Serrano M, Pérez-Pérez R, Sabater M, Ricart W, et al.Decreased STAMP2 expression in association with visceral adipose tissue dysfunction. J Clin Endocrinol Metab2011;96:E1816–E1E25. [PubMed: 21849520]

[17]. Tsuchida A, Yamauchi T, Takekawa S, Hada Y, Ito Y, Maki T, et al.Peroxisome Proliferator–Activated Receptor (PPAR)α activation increases adiponectin receptors and reduces obesity-related inflammation in adipose tissue. Diabetes2005;54:3358. [PubMed: 16306350]

[18]. Stienstra R, Duval C, Keshtkar S, van der Laak J, Kersten S, Muller M. Peroxisome proliferator-activated receptor g activation promotes infiltration of alternatively activated macrophages into adipose tissue. J Biol Chem2008;283:22620–7. [PubMed: 18541527]

[19]. Lehmann JM, Moore LB, Smith-Oliver TA, Wilkison WO, Willson TM, Kliewer SA. An antidiabetic thiazolidinedione is a high affinity ligand for peroxisome proliferator-activated receptor g (PPAR g). J Biol Chem1995;270:12953–6. [PubMed: 7768881]

[20]. Berger J, Bailey P, Biswas C, Cullinan C, Doebber T, Hayes N, et al.Thiazolidine-diones produce a conformational change in peroxisomal proliferator-activated receptor-gamma: binding and activation correlate with antidiabetic actions in db/db mice. Endocrinology1996;137:4189–95. [PubMed: 8828476]

[21]. Chao L, Marcus-Samuels B, Mason MM, Moitra J, Vinson C, Arioglu E, et al.Adipose tissue is required for the antidiabetic, but not for the hypolipidemic, effect of thiazolidinediones. J Clin Invest2000;106:1221–8. [PubMed: 11086023]

[22]. Sugii S, Olson P, Sears DD, Saberi M, Atkins AR, Barish GD, et al.PPARg activation in adipocytes is sufficient for systemic insulin sensitization. Proc Natl Acad Sci USA. 2009;106:22504–9. [PubMed: 20018750]

[23]. Huo Y, Guo X, Li H, Wang H, Zhang W, Wang Y, et al.Disruption of inducible 6-phosphofructo-2-kinase ameliorates diet-induced adiposity but exacerbates systemic insulin resistance and adipose tissue inflammatory response. J Biol Chem2010;285:3713–21. [PubMed: 19948719]

[24]. Xu H, Li H, Woo S-L, Kim S-M, Shende VR, Neuendorff N, et al.Myeloid cell-specific disruption of Period1 and Period2 exacerbates diet-induced inflammation and insulin resistance. J Biol Chem2014;289:16374–88. [PubMed: 24770415]

[25]. Pei Y, Li H, Cai Y, Zhou J, Luo X, Ma L, et al.Regulation of adipose tissue inflammation by adenosine 2A receptor in obese mice. J Endocrinol2018;239:365–76. [PubMed: 30400017]

[26]. Huo Y, Guo X, Li H, Xu H, Halim V, Zhang W, et al.Targeted overexpression of inducible 6-phosphofructo-2-kinase in adipose tissue increases fat deposition but protects against diet-induced insulin resistance and inflammatory responses. J Biol Chem2012;287:21492–500. [PubMed: 22556414]

[27]. Chesney J, Telang S, Yalcin A, Clem A, Wallis N, Bucala R. Targeted disruption of inducible 6-phosphofructo-2-kinase results in embryonic lethality. Biochem Biophys Res Commun2005;331:139–46. [PubMed: 15845370]

[28]. Luo X, Li H, Ma L, Zhou J, Guo X, Woo S-L, et al.Expression of STING is increased in liver tissues from patients with NAFLD and promotes macrophage-mediated hepatic inflammation and fibrosis in mice. Gastroenterology2018;155:1971–84. [PubMed: 30213555]

[29]. Ma L, Li H, Hu J, Zheng J, Zhou J, Botchlett R, et al.Indole alleviates diet-induced hepatic steatosis and inflammation in a manner involving myeloid cell PFKFB3. Hepatology2020n/a: [Epub ahead of print].

[30]. Guo X, Li H, Xu H, Halim V, Zhang W, Wang H, et al.Palmitoleate induces hepatic steatosis but suppresses liver inflammatory response in mice. PLoS ONE2012;7:e39286. [PubMed: 22768070]

[31]. Cai Y, Li H, Liu M, Pei Y, Zheng J, Zhou J, et al.Disruption of adenosine 2A receptor exacerbates NAFLD through increasing inflammatory responses and SREBP1c activity. Hepatology2018;68:48–61. [PubMed: 29315766]

[32]. Guo T, Woo S-L, Guo X, Li H, Zheng J, Botchlett R, et al.Berberine ameliorates hepatic steatosis and suppresses liver and adipose tissue inflammation in mice with diet-induced obesity. Sci Rep2016;6:22612. [PubMed: 26936230]

[33]. Çimen I, Kocatürk B, Koyuncu S, Tufanli Ö, Onat UI, Yıldırım AD, et al.Prevention of atherosclerosis by bioactive palmitoleate through suppression of organelle stress and inflammasome activation. Sci Transl Med2016;8358ra126.

[34]. Chan KL, Pillon NJ, Sivaloganathan DM, Costford SR, Liu Z, Théret M, et al.Palmitoleate reverses high fat-induced proinflammatory macrophage polarization via AMP-activated Protein Kinase (AMPK). J Biol Chem2015;290:16979–88. [PubMed: 25987561]

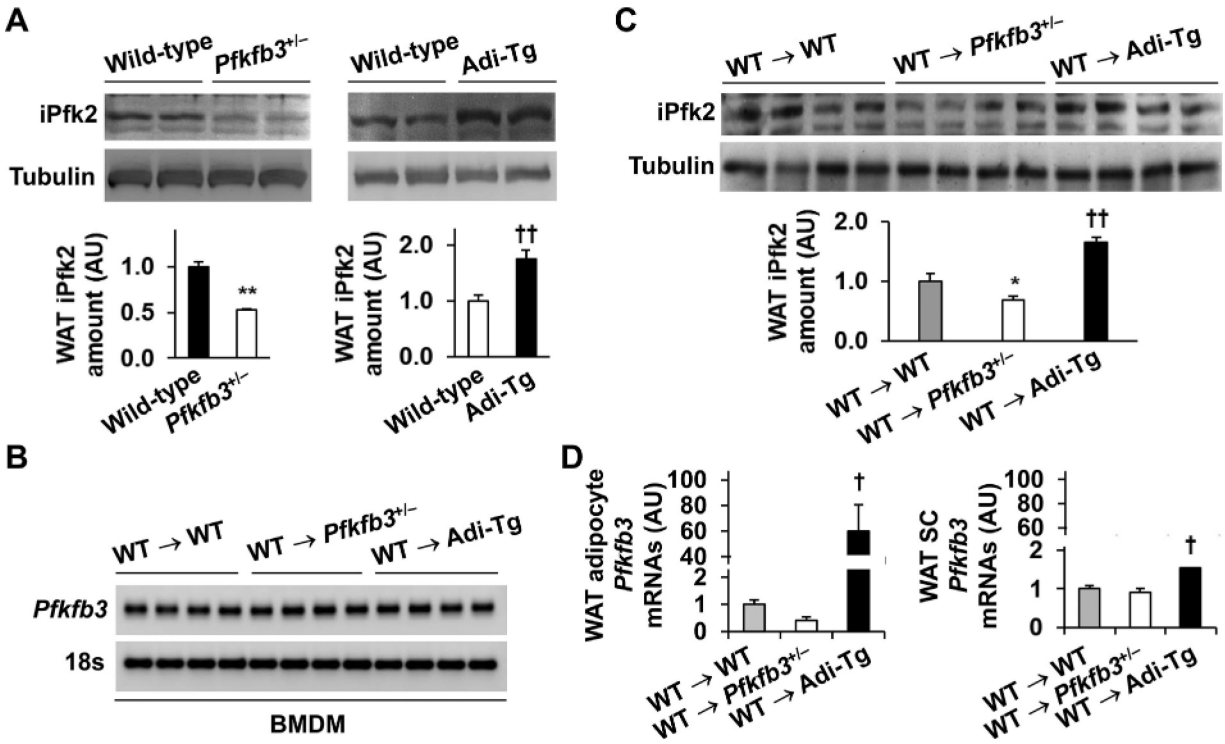

Fig. 1.

Adoptive transfer of wild-type hematopoietic cells to recipients does not alter adipose tissue amount of iPk2. (A) White adipose tissue iPfk2 amount. *Pfkfb3*-disrupted (*Pfkfb3*$^{+/-}$) mice and wild-type (WT) littermates, as well as adipocyte-specific *Pfkfb3*-overexpressing (Adi-Tg) mice and WT littermates, were maintained on a chow diet. At 10–12 wk of age, male mice were harvested to examine iPfk2 amount in white adipose tissue (WAT) using Western blot analysis. Top panels, representative blots from WAT of 2 mice per group. Bottom panel, quantification of blots. n=4 (wild type) or 6 (*Pfkfb3*$^{+/-}$ or Adi-Tg). (B) *Pfkfb3* mRNA levels in bone marrow-derived macrophages (BMDMs) from chimeric mice. Representative images. (C) The iPfk2 amount in WAT from chimeric mice. (D) *Pfkfb3* expression in WAT adipocytes and stromal cells. For B–D, male WT, *Pfkfb3*$^{+/-}$, and Adi-Tg mice, at 5–6 wk of age, were lethally irradiated and transplanted with bone marrow cells from WT C57BL/6J mice. After bone marrow transplantation, chimeric mice were fed a high-fat diet (HFD, 60% of fat calories) for 12 wk. After harvest, BMDMs (B) and lysates of WAT (C) were examined for *Pfkfb3* mRNA levels and iPfk2 amount, respectively. Also, adipocytes and stromal cells were isolated from WAT in chimeric mice and subjected to analysis of *Pfkfb3* mRNA levels (D). n=5–7. WT → WT mice, WT mice transplanted with WT hematopoietic cells; WT → *Pfkfb3*$^{+/-}$ mice, global *Pfkfb3*-disrupted mice transplanted with WT hematopoietic cells; WT → Adi-Tg mice, adipocyte-specific *Pfkfb3*-overexpressing mice transplanted with WT hematopoietic cells. For C, top panels, representative blots for WAT lysates from 4 individual mice per group. Bottom panel, quantification of blots. n=7. For bar graphs in A, C, and D, data are means ± SEM. *, $P < 0.05$ and **, $P < 0.01$ *Pfkfb3*$^{+/-}$ vs. WT in A or WT → *Pfkfb3*$^{+/-}$ vs. WT → WT in C; †, $P < 0.05$ and ††, $P < 0.01$ Adi-Tg vs. WT in A or WT → Adi-Tg vs. WT → WT in C and D.

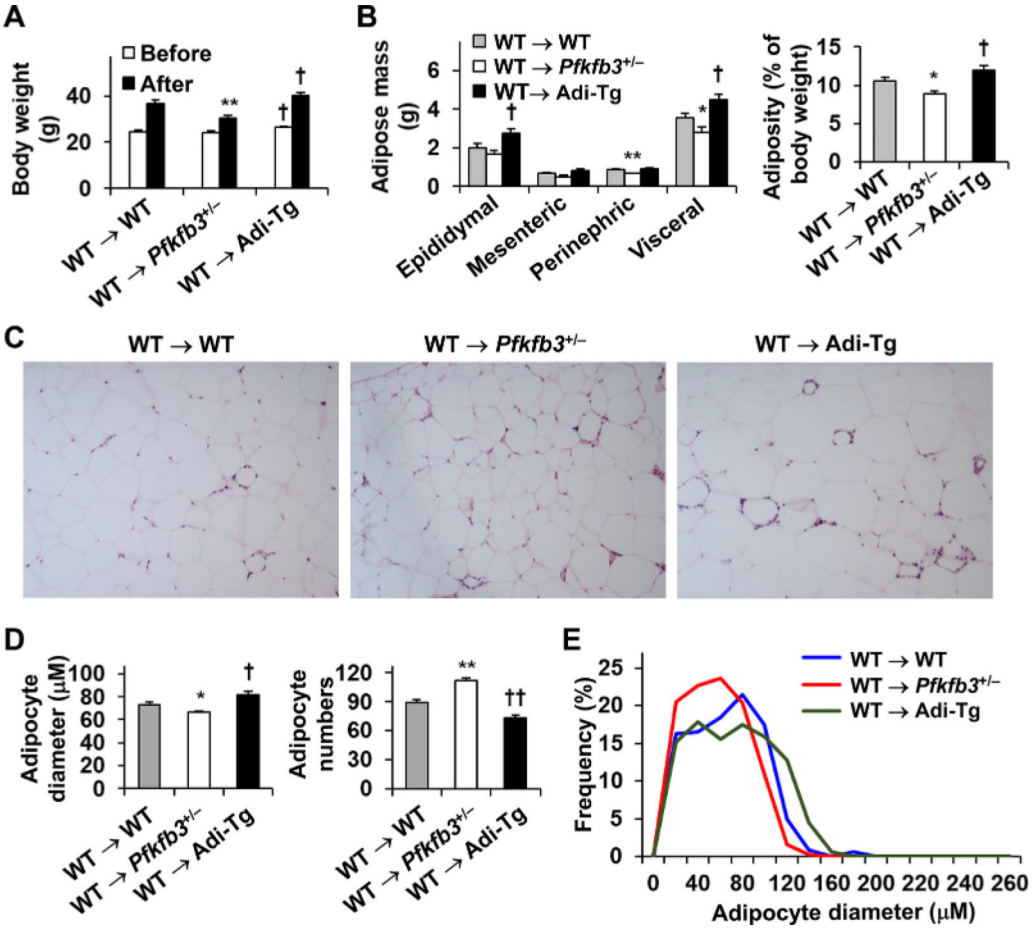

Fig. 2.

The iPfk2 in adipocytes, but not hematopoietic cells, determines body weight and adiposity. (A) Body weight of chimeric mice before and after HFD feeding. (B) Abdominal fat mass and adiposity of chimeric mice after the feeding period. (C) WAT histology of chimeric mice after HFD feeding. (D) WAT adipocyte size and number. A total of 8–10 randomized fields of histology images for WAT from a subtotal of 5–7 mice per group were analyzed. (E) WAT adipocyte distribution. Adipocyte frequency was plotted based on the numbers of adipocytes within a given diameter range of size. For A–E, chimeric mice were generated as described in Fig. 1. After recovery from BMT for 4 wk, the mice were fed an HFD for 12 wk. For A, B, and D, data are means ± SEM. For A and B, n=7 (adipose mass and adiposity) or 10 (body weight). *, $P < .05$ and **, $P < .01$ WT → *Pfkfb3*$^{+/-}$ vs. WT → WT in A after HFD feeding, in B for the same type of fat or adiposity, and in D for adipocyte size or number. †, $P < .05$ WT → Adi-Tg vs. WT → WT in A before or after HFD feeding, in B for the same type of fat or adiposity, and in D for adipocyte size or number.

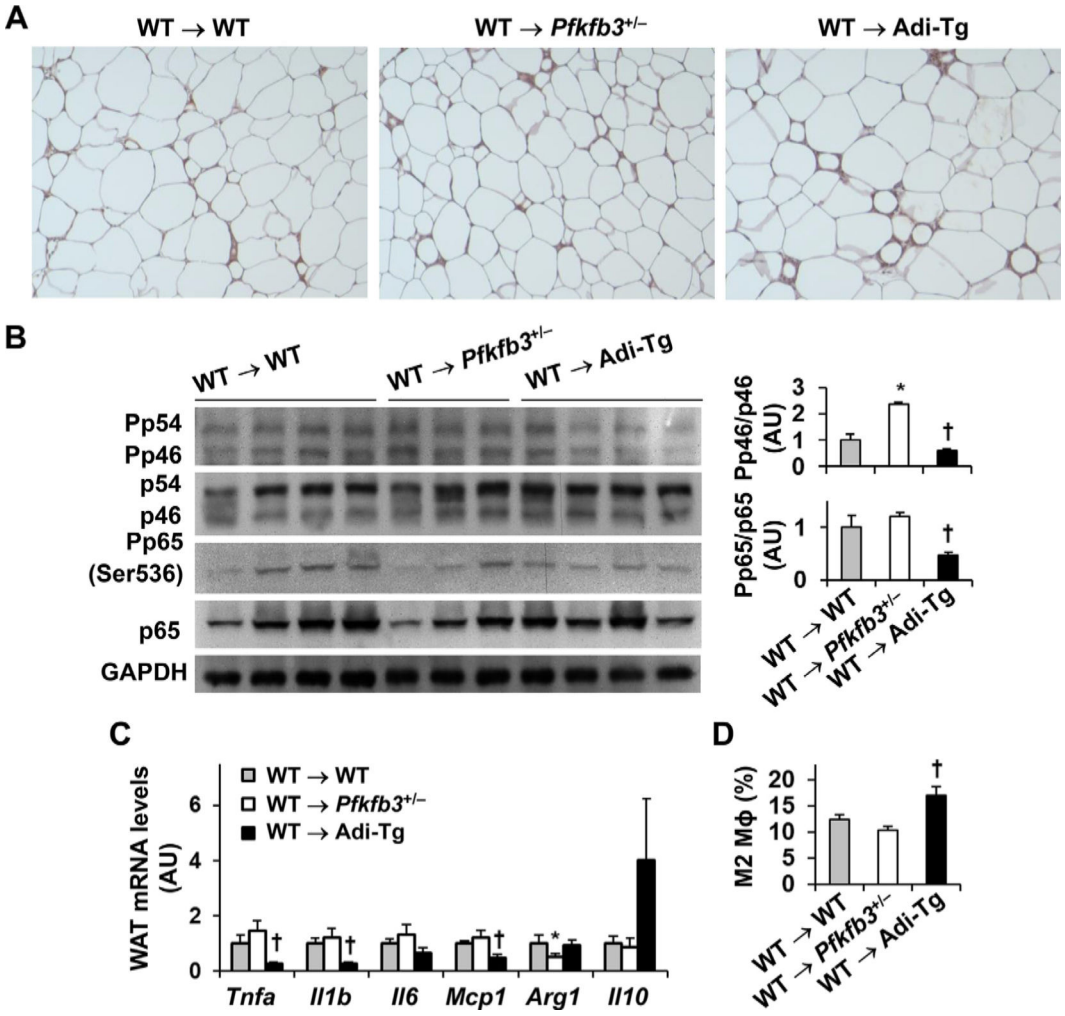

Fig. 3.

Adoptive transfer of wild-type hematopoietic cells to recipients does not weaken the effect of aP2-driven *Pfkfb3* overexpression on ameliorating the severity of HFD-induced WAT inflammation. (A) WAT macrophage infiltration. (B) WAT proinflammatory signaling. (C) WAT expression of genes for cytokines and inflammatory mediators. (D) WAT macrophage alternative (M2) activation. For A–D, chimeric mice were generated as described in Fig. 1 and fed an HFD for 12 wk. For A, WAT sections were stained for F4/80 expression. For B, WAT lysates were subjected to Western blot analysis. Left panels, representative blots from 3–4 WAT per group. Bar graphs, quantification of blots for all WAT samples. n=7. For C, WAT RNA was subjected to reverse transcription and real-time PCR. n=7. For D, WAT macrophage alternative activation was examined using FACS analysis. Stromal cells isolated from WAT in chimeric mice were analyzed for mature macrophages ($F480^+$ $CD11b^+$ cells), which were further analyzed for M2 macrophages ($CD206^+$ $CD11c^-$ cells). n=5–7. For bar graphs in B,C, and D, data are means ± SEM. *, $P < .05$ WT → *Pfkfb3*$^{+/-}$ vs. WT → WT for the same protein (B) or gene (C); †, $P < .05$ WT → Adi-Tg vs. WT → WT for the same protein (B), gene (C), or macrophage type (D).

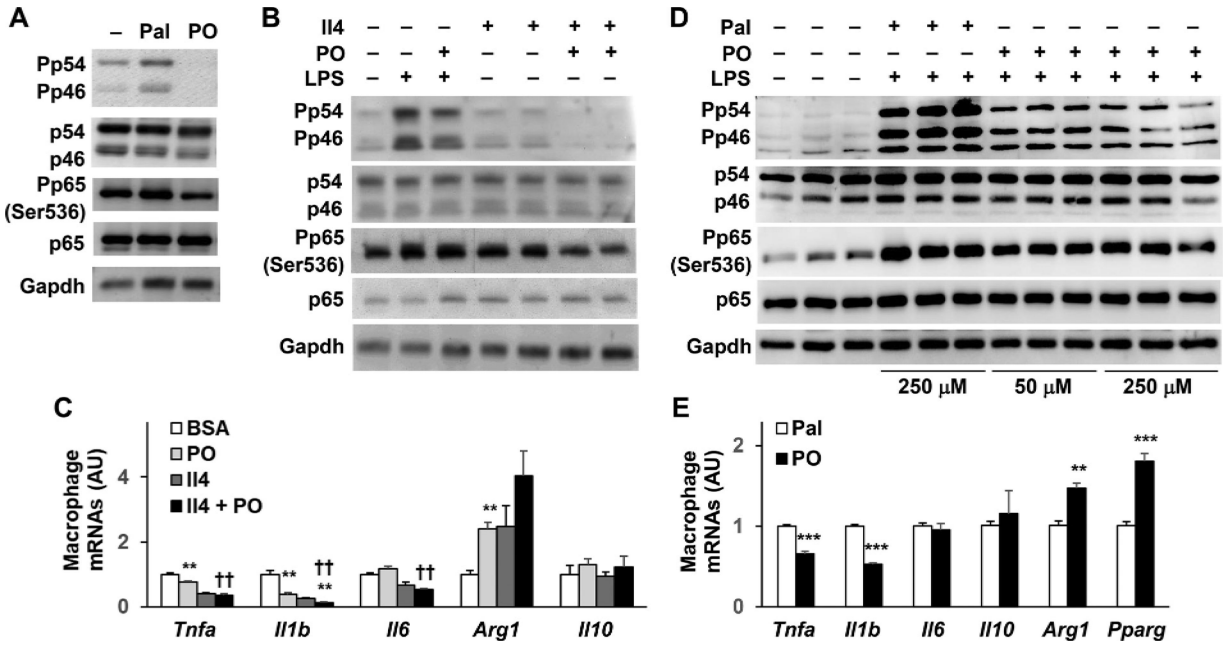

Fig. 4.

Palmitoleate, a *Pfkfb3*-driven adipocyte bioactive lipid, promotes macrophage anti-inflammatory activation. (A,B,C,D,E) Palmitoleate regulates macrophage activation status. For A, WT BMDMs were supplemented with palmitoleate (PO, 50 μM) or palmitate (Pal, 250 μM) for 24 hr. For B and C, WT BMDMs were treated with interleukin 4 (Il4, 10 ng/mL) for 48 h and supplemented with or without PO (50 μM) for the last 24 hr. For D, WT BMDMs were supplemented with PO (50 or 250 μM) or Pal (250 μM) for 24 h in the presence or absence of LPS (100 ng/mL) for the last 30 min. For E, WT BMDMs were supplemented with PO (250 μM) or Pal (250 μM) for 24 hr. For A,B, and D, cell lysates were subjected to Western blot analysis. For C and E, the expression of genes for cytokines and inflammatory mediators in BMDMs were analyzed using real-time POL For C and E, data are means ± SEM. n=6–8. *, $P < 0.05$, **, $P < .01$, and ***, $P < .001$ PO vs. BSA or Il4 + PO vs. Il4 in C or PO vs. Pal in E for the same gene; ††, $P < .01$ Il4 + PO vs. PO in C for the same gene.

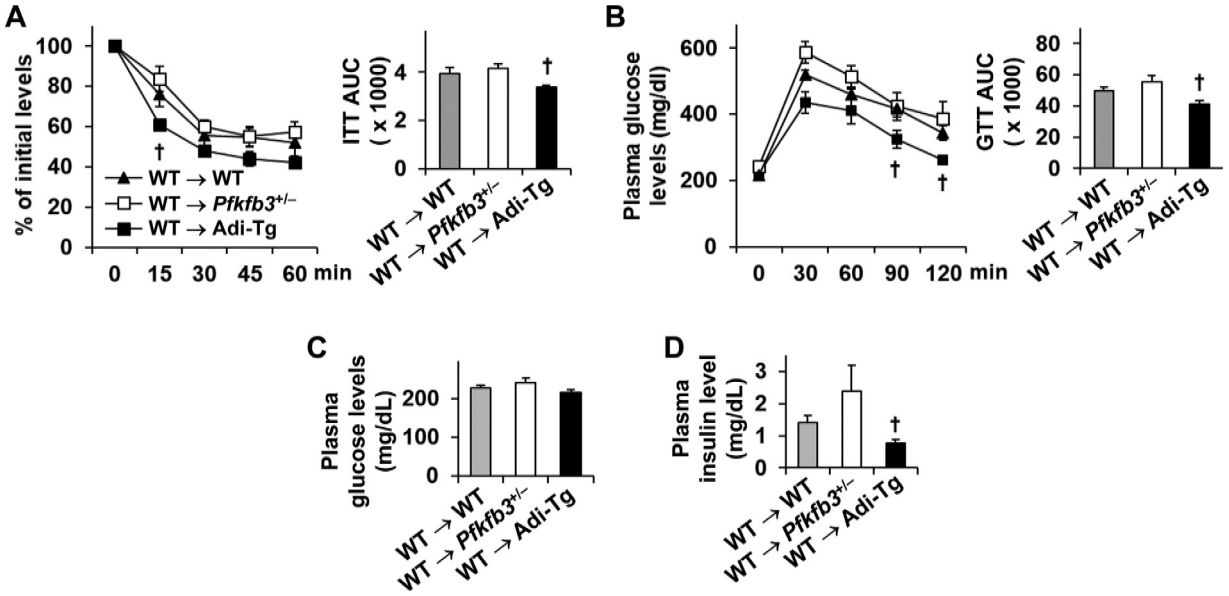

Fig. 5.

Adoptive transfer of wild-type hematopoietic cells to recipients does not weaken the effect of aP2-driven *Pfkfb3* overexpression on ameliorating the severity of HFD-induced insulin resistance and glucose intolerance. (A,B) Insulin sensitivity and glucose tolerance tests in chimeric mice. Bar graphs, AUC based on insulin and glucose tolerance tests. (C) Plasma levels of glucose. (D) Plasma levels of insulin. For A–D, chimeric mice were generated as described in Fig. 1 and fed an HFD for 12 wk. After the feeding period, the mice were fasted for 4 h and subjected to an intraperitoneal injection of insulin (1 U/kg body weight) or glucose (2 g/kg body weight). For C and D, chimeric mice were fasted for 4 h prior to harvest of blood samples. For A–D, data are means ± SEM. n=10. †, P < .05 WT → Adi-Tg vs. WT → WT in line graphs of A and B for the same time point or in bar graphs of A, B, and D.

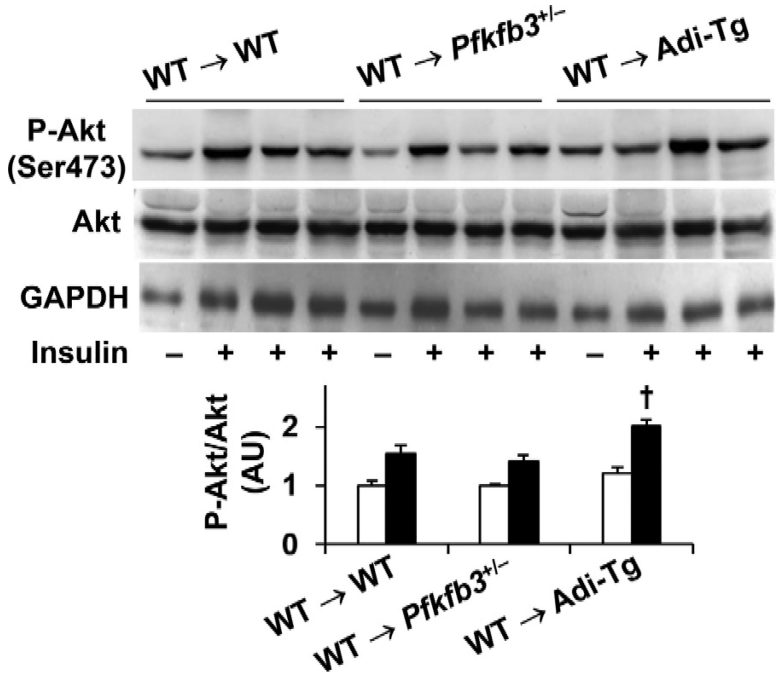

Fig. 6.

Adoptive transfer of wild-type hematopoietic cells to recipients maintains the effect of aP2-driven *Pfkfb3* overexpression on increasing WAT insulin signaling. WAT insulin signaling in chimeric mice. After the feeding period, chimeric mice (described in Fig. 1) were fasted for 4 h and subjected to a bolus injection of insulin (1 U/kg body weight) into the portal vein for 5 min. WAT lysates were examined for the total amount and phosphorylation states of Akt using Western blot analysis. Top panels, representative blots. Bottom panel, quantification of blots. Data are means ± SEM. n=4 (without insulin) or 6 (with insulin). †, $P < .05$ WT → Adi-Tg vs. WT → WT under insulin-stimulated condition.